ELSEVIER

Chemical Engineering Journal 91 (2003) 33–44

Chemical Engineering Journal

www.elsevier.com/locate/cej

Mass transfer behaviour of a flow-by fixed bed electrochemical reactor under different hydrodynamic conditions

E.A. Soltan, S.A. Nosier, A.Y. Salem, I.A.S. Mansour, G.H. Sedahmed*

Department of Chemical Engineering, Faculty of Engineering Alexandria University, Alexandria, Egypt

Received 2 November 2001; accepted 6 April 2002

Abstract

Mass transfer behaviour of a flow-by electrode made of a fixed bed of Raschig rings and cylinders supported by a vertical plate feeder electrode was studied. The rate of mass transfer of the bed–plate assembly was determined under single phase, gas sparging and two phase flow-by measuring the limiting current of the cathodic deposition of copper from acidified copper sulphate solutions. Variables studied were: particle diameter, height of bed–plate assembly, physical properties of the solution, superficial gas velocity, superficial solution velocity. The data under different conditions were correlated by dimensionless equations. Although the mass transfer coefficient of the bed electrode is less than that of the plate electrode, it was found that the volumetric mass transfer coefficient of the bed electrode and hence its productivity is higher than that of the plate electrode by a factor which ranges from 2.8 to 9.6 depending on the operating conditions. Power consumption calculation has shown that for a given set of conditions, bed electrodes consume less electrical energy in kWh/kg than the plate electrode under different flow conditions.

Keywords: Fixed bed; Mass transfer; Copper deposition electrochemical reactor

1. Introduction

During the last few decades, the performance characteristics of the fixed bed electrochemical reactor such as mass transfer and current distribution have been the subject of many investigations in view of its high space time yield and its ability to handle efficiently diffusion controlled reactions, involving dilute solutions such as those encountered in electroorganic synthesis and electrochemical waste-water treatment. These studies came to the conclusion that flow-through fixed bed electrodes where the current and solution flow are parallel suffer from the non-uniformity of potential and current distribution [1]. It was suggested that this drawback can be overcome by using a multistage flow-through fixed bed electrochemical reactor, each stage consists of a thin horizontal fixed bed working electrode located between two horizontal counter electrodes, an upstream and a downstream counter electrode made of metallic screen [2,3].

Alternatively, to obtain uniform current and potential distribution, the fixed bed electrode should be operated in the flow-by regime where current and solution flow are perpendicular [1]. Previous mass transfer studies on flow-by fixed bed electrode, were carried out using graphite particles, stacks of parallel screens or expanded metal, carbon felt and foam [1]. Although the active specific area and the space time yield of these electrode material are high, they suffer from the high pressure drop and tendency to clogging especially when used to remove heavy metals from industrial waste solutions. Besides, fixed bed electrodes made of small particles, metal felt and metal foam may entrap gas bubbles (H_2 or O_2) which are likely to evolve simultaneously with the main reactions from dilute solutions with a consequent increase in cell resistance and electrical energy consumption [1]. Moreover, such low porosity electrodes are difficult to operate under gas sparging or two phase flow which is sometimes essential as in the case of H_2O_2 synthesis [4], flue gas desulphurization [5] and alkene oxide production [6].

The aim of the present work, is to examine the mass transfer behaviour of a flow-by fixed electrode built of relatively large Raschig rings, and cylinders under different flow conditions such as single phase flow, gas sparging and two phase flow. Although, large particles give less active specific area and lower space time yield than small packing material they are expected to suffer less from pressure drop, clogging and entrapment of gas bubbles in case of metal deposition from waste solutions. Rates of mass transfer were determined under different conditions by measuring the limiting current of the cathodic deposition of copper from

* Corresponding author.

1385-8947/02/$ – see front matter
PII: S1385-8947(02)00083-9

Nomenclature

a, a_1	constant
A	electrode area
A_p	particle area
C	concentration of Cu^{++} in the solution
d	Raschig ring or cylinder diameter
d_e	equivalent diameter of the cell $d_e = 4 \times$ cross-sectional area/wetted perimeter
D	diffusivity
D_p	equivalent particle diameter
F	Faraday's constant
Fr	Froude number (V_g^2/hg) for the plate electrode and (V_g^2/dg) for the bed electrode
g	acceleration due to gravity
h	electrode height (plate or bed)
I	limiting current
J	mass transfer J factor ($St{\cdot}Sc^{0.66}$)
K	mass transfer coefficient
K_o and K_{eff}	specific conductivity of the solution and bed-solution, respectively
L	bed equivalent diameter defined by Eq. (8)
R	cell resistance
Re	solution Reynolds number ($\rho Vh/\mu$) for the plate electrode and ($\rho Vd/\mu$) for bed electrode
Re_g	gas Reynolds number ($\rho V_g h/\mu$) for the plate electrode and ($\rho V_g d/\mu$) for bed electrode
Sc	Schmidt number ($\mu/\rho D$)
St	Stanton number (K/V) in case of single phase flow and (K/V_g) in case of gas sparging
Sh	Sherwood number (Kh/D) for the plate electrode and (Kd/D) for the bed electrode
V	superficial solution velocity
V_g	superficial gas velocity
Z	number of electrons involved in the reaction
Greek letters	
ε	bed porosity
μ	solution viscosity
ρ	solution density

acidified copper sulphate, special attention was given to low solution velocities which have the advantage of increasing the residence time and the degree of conversion per pass.

A single related study was conducted by Pickett and Stanmore [7] who measured rates of single phase mass transfer at a flow-by single layer of spheres, each sphere had 6.35 mm diameter. The authors correlated their data for the conditions $23 < Re < 520$ by the equation:

$$Sh = 0.83 Sc^{0.33} Re^{0.56} \quad (1)$$

Particle diameter was used as a characteristic length in calculating Sh and Re. Variation of electrode potential throughout the bed were found to be small enough to ensure reaction selectivity.

For the purpose of evaluating the performance of the bed–plate assembly in comparison with the plate electrode, the mass transfer behaviour of the plate electrode was also studied under the present range of conditions where single phase laminar flow and low gas velocities were used. The present range of conditions differ from those previously used to study the mass transfer behaviour of the plate electrode under gas sparging [8,9] and two phase flow [10,11].

2. Experimental technique

The apparatus (Fig. 1) consisted of the cell, electrical circuit and flow circuit. The cell was a plexiglass rectangular container of 30 cm height, the base of the cell was perforated plexiglass plate of the dimensions 6 cm × 7 cm, the upstream

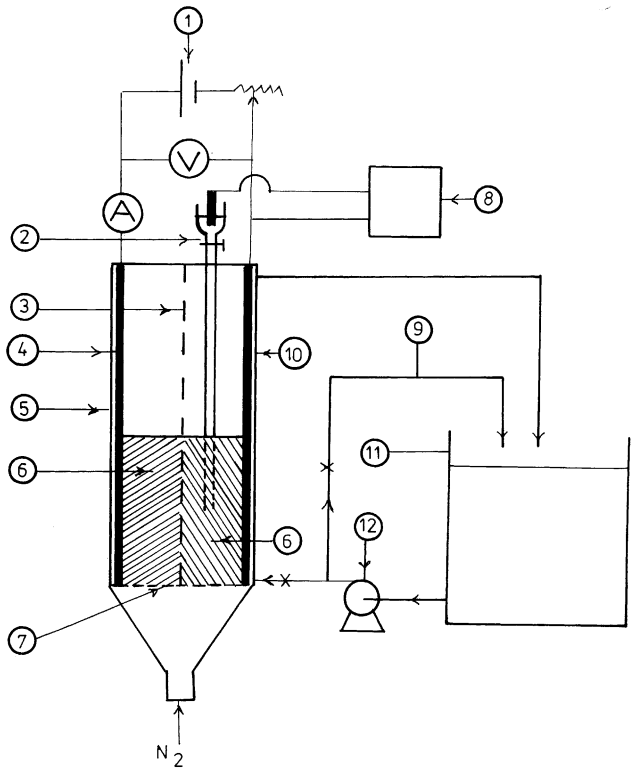

Fig. 1. Apparatus: (1) volt dc power supply; (2) Luggin tube with a $Cu/CuSO_4$ reference electrode; (3) perforated plastic separator; (4) fixed bed feeder (copper plate); (5) plexiglass cell; (6) Raschig rings or cylinder packing; (7) gas distributor; (8) high impedance voltmeter; (9) bypass; (10) fixed bed cathode feeder; (11) 30 l plexiglass storage tank; (12) 0.25 hp plastic centrifugal pump.

side of the plate was covered with thick cloth to increase the pressure drop and ensure uniform gas distribution. The cell was divided into two compartments by a rigid plastic screen of square openings (2 mm × 2 mm) to avoid contact between the cathodic bed and anodic bed. A copper plate cathode and a copper plate anode each having a height of 30 cm and a width of 6 cm were placed at the opposite cell walls. The rigid plastic screen separator and the two copper electrodes were fixed in position by inserting their edges in vertical grooves machined in the side walls of the cell. Fixed bed–plate assembly electrode was built by packing the cathode and anode compartments with copper Raschig rings or cylinders arranged at random and well compacted, the plate acted as a current feeder for the fixed bed. The maximum active height of the plate electrode as well as the bed was limited to 12 cm, the backs of the two feeder plates facing the cell walls as well as the undesired area were isolated with epoxy resin. Copper Raschig rings and copper cylinders of diameters 0.6, 0.8 and 1 cm were used in building the fixed beds, in all cases the aspect ratio was 1, equivalent particle diameter d_p is shown in Table 1. Four active plate and bed heights were used: 6, 8, 10 and 12 cm. The number of rings or cylinders used to build a fixed bed electrode of 6 cm width and 3.5 cm depth ranged from 62 to 650 depending on particle size and bed height, the porosity of different beds are shown in Table 1. The plastic screen partition served to avoid contact between the cathodic and anodic packing.

To study the rate of mass transfer under forced convection and two phase flow, solution was circulated by means of 0.25 hp plastic centrifugal pump between 30 l plexiglass storage tank and the cell. Solution flow rate was controlled with a bypass and was measured by a stopwatch and a graduated cylinder. To study the rate of mass transfer under gas sparging and two phase flow nitrogen gas was introduced to the cell from a N_2 cylinder through the perforated bottom. Gas flow rate was measured by means of a calibrated U tube manometer. In case of gas sparging, a cell with an open top was used. The electrical circuit consisted of 12 V dc power supply with a voltage regulator and a multirange ammeter connected in series with the cell. A voltmeter was connected in parallel with the cell to measure its voltage.

The limiting current of the cathodic deposition of copper under different conditions was measured by increasing the current stepwise and measuring the steady state cathode potential against a reference electrode by means of a high impedance voltmeter. The reference electrode consisted of a copper wire placed in the cup of plastic Luggin capillary tube filled with a solution identical with the cell solution. The tip of the Luggin capillary was embedded in the middle of the fixed bed; in case of the plate electrode, the tip of the Luggin capillary was positioned at the middle of the electrode 0.5–1 mm from its surface. In case of gas sparging and two phase flow, a cotton plug was inserted inside the Luggin tip to prevent gas bubbles from entering inside the capillary. Solutions used in the present study contained xM $CuSO_4$ in 1 M H_2SO_4, x ranged from 0.0125 to 0.1 M. All solutions were prepared from A.R. grade chemicals and distilled water. $CuSO_4$ concentration was checked by iodometry [12]. Solution viscosity and density were determined by an Ostwald viscomter and density bottle, respectively [13]. Diffusivity of Cu^{++} was calculated from the equation [14]:

$$\frac{D\mu}{T} = [1.98 + 2.34C_{Cu^{++}}] \times 10^{-10} \text{ (dyn/°K)} \quad (2)$$

Experiments were carried out in the temperature range 18–22 °C, temperature was measured in each experiment and the physical properties were determined accordingly.

3. Results and discussion

3.1. Mass transfer under single phase flow

Polarization curves with a well defined limiting current plateau (Fig. 2) were obtained for different electrodes under the different hydrodynamic conditions used in the present study, the limiting current obtained from these curves was used to calculate the mass transfer coefficient according to the equation [14]:

$$K = \frac{I}{ZFAC} \quad (3)$$

In case of the bed–plate assembly, the electrode area A was obtained by adding the active feeder plate area to the bed area which was calculated by multiplying the number of particles by the particle area.

The mass transfer coefficient was related to other variables for the plate electrode, a bed of Raschig rings–plate assembly and a bed of cylinders–plate assembly using the dimensionless groups *Sh*, *Sc* and *Re*, in case of bed–plate combination an extra dimensionless group was found necessary to account for the effect of bed height, namely(d/h).

Table 1
Bed parameters at different ring and cylinder diameters

d_{ring} (cm)	d_p (cm)	ε	L (cm)	$d_{cylinder}$ (cm)	d_p (cm)	ε	L (cm)
0.6	0.848	0.685	0.87	0.6	0.735	0.5	0.4
0.8	1.131	0.785	1.95	0.8	0.980	0.65	0.87
1	1.41	0.87	4.46	1	1.225	0.62	1.09

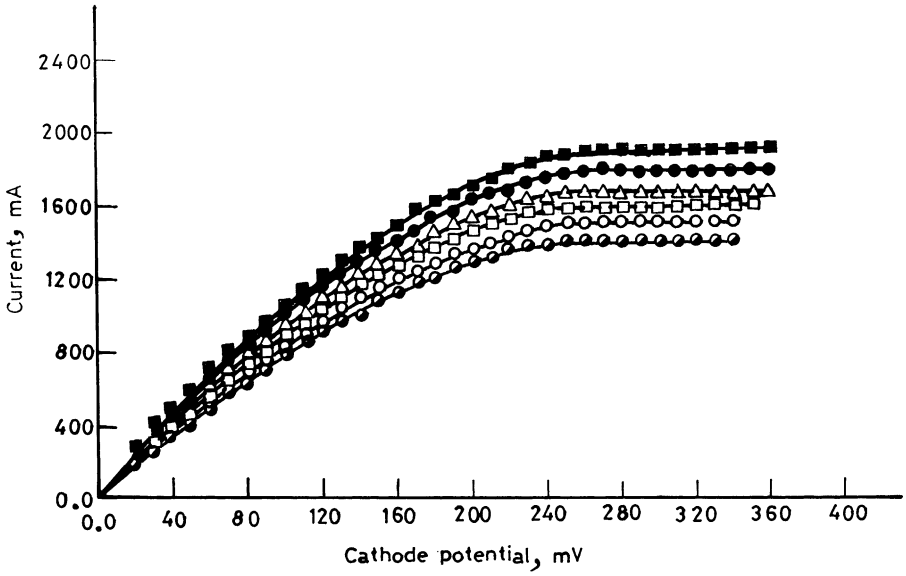

Fig. 2. Typical polarization curves obtained for fixed bed of Raschig rings–plate assembly under single phase flow. $CuSO_4$ conc., 0.05 M; ring diameter, 0.8 cm; bed height, 6 cm; superficial solution velocity (cm/s): (◑) 0.684; (○) 1.15; (□) 1.46; (△) 1.78; (●) 2.1; (■) 2.51.

Fig. 3 shows that the mass transfer data at a vertical plate in an empty channel for the conditions $1918 < Sc < 2026$, $350 < Re < 2666$, fit the equation:

$$Sh = 0.625Sc^{0.33}Re^{0.55} \quad (4)$$

With an average deviation of ±12.4%, *Sh* and *Re* were calculated using plate height as a characteristic length. Eq. (4) is in a fair agreement with the equation obtained using the hydrodynamic boundary layer theory for mass transfer at a flat plate under developing laminar flow conditions [14].

$$Sh = 0.67Sc^{0.33}Re^{0.55} \quad (5)$$

Fig. 4 shows that the mass transfer data for fixed bed of Raschig rings–plate assembly under single phase flow for the conditions $1546 < Sc < 1729$, $38 < Re < 231$ and $0.05 < d/h < 0.167$, fit the equation:

$$J = 3.85Re^{-0.72}\left(\frac{d}{h}\right)^{0.72} \quad (6)$$

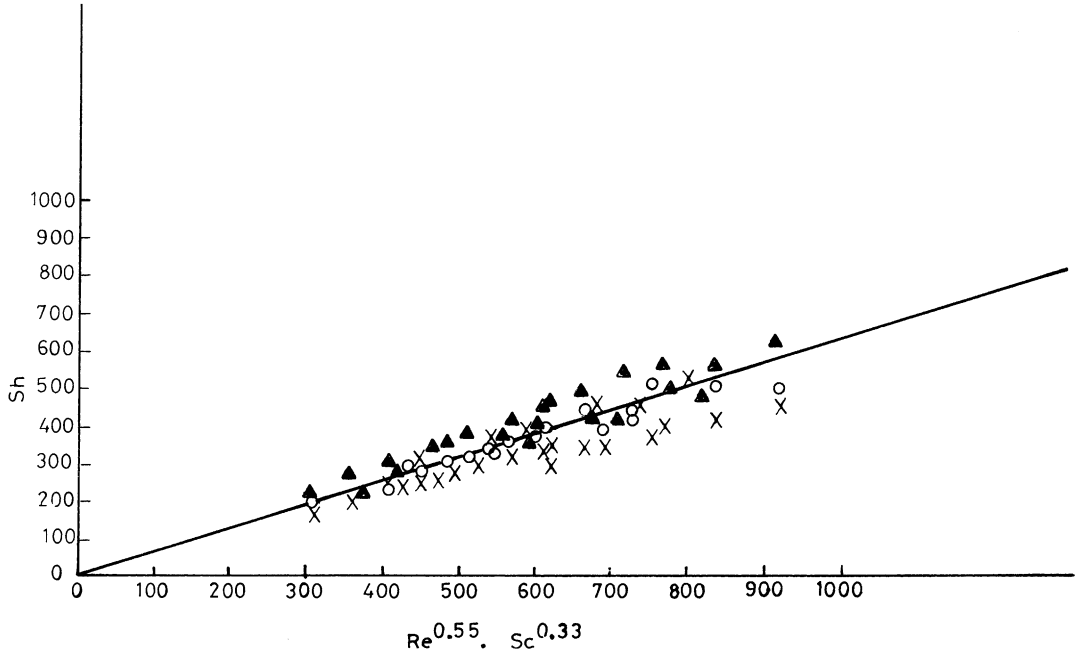

Fig. 3. Mass transfer correlation at a vertical plate under single phase flow. *Sc*: (○) 1884; (X) 1918; (▲) 2025.

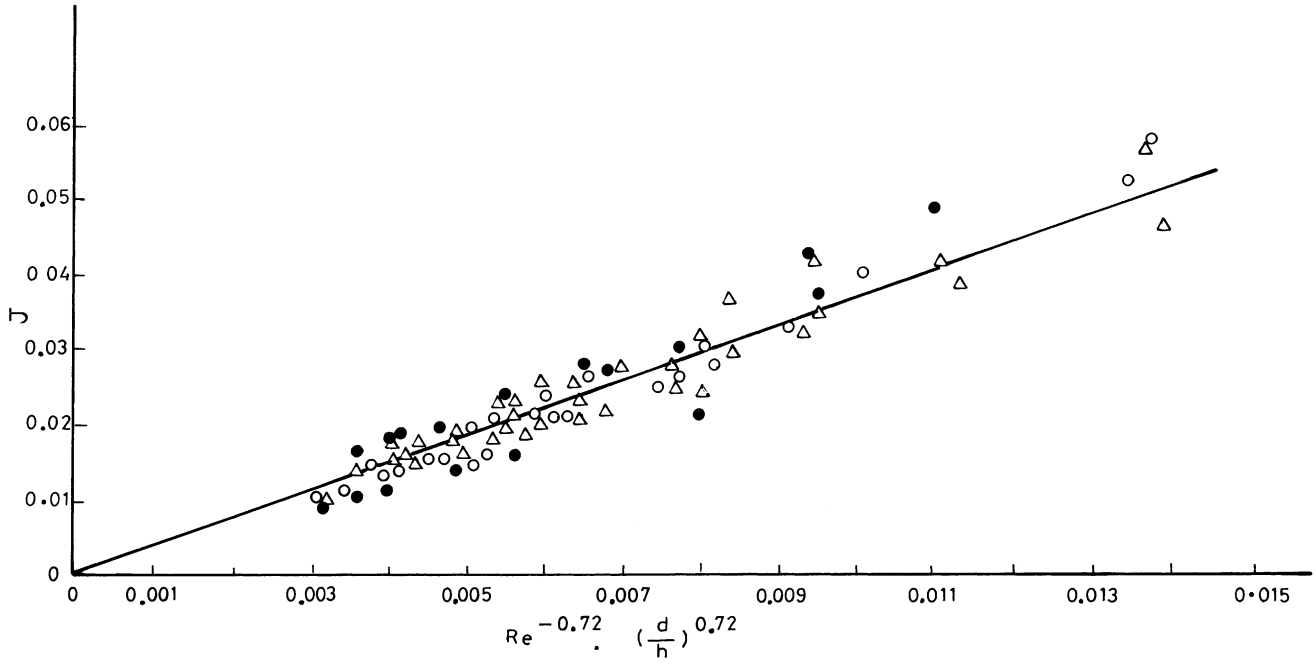

Fig. 4. Mass transfer correlation at a fixed bed of Raschig rings–plate assembly electrode under single phase flow. *Sc*: (○) 1546; (●) 1697; (△) 1729.

with an average deviation of ±9.8%. For simplicity, *Re* was calculated using ring diameter as a characteristic length. Eq. (6) can be also written in the form:

$$Sh = 3.85Sc^{0.33}Re^{0.28}\left(\frac{d}{h}\right)^{0.72} \quad (7)$$

To compare the present data with previous related studies, the data were also correlated using the bed equivalent diameter L given by

$$L = \frac{4 \times \text{void volume}}{\text{wetted surface area}} = \frac{2\varepsilon d_p}{3(1-\varepsilon)} \quad (8)$$

as a characteristic length, d_p is the equivalent particle diameter $\left(d_p = \sqrt{A_p/\pi}\right)$. An equation similar to Eq. (6) was obtained but with a coefficient of 6.85 instead of 3.85, the average deviation was ±14.9%. Eq. (6) shows that under the present conditions, ring diameter has a negligible effect on the mass transfer coefficient while increasing bed height leads to decreasing the mass transfer coefficient according to the equation:

$$K = ah^{-0.72} \quad (9)$$

The decrease in mass transfer coefficient with increasing bed–plate assembly height may be attributed to the following effects:

(i) since the feeder plate is an integral part of the bed–plate assembly, it is probable that the build up of a developing hydrodynamic boundary layer and diffusion layer along the vertical plate contributes to the decrease in mass transfer with increasing bed height;

(ii) decrease of copper ion concentration as the solution progresses through the bed; replenishment of the depleted copper ions from the dissolving copper anode seems to be hindered by flow maldistribution in the bed which is likely to take place under the present conditions where relatively thin bed of large particles is used [15].

Fig. 5 shows that the mass transfer data for a fixed bed of cylinders–plate assembly under single phase flow for the conditions $1729 < Sc < 1918$, $38 < Re < 220$ and $0.05 < d/h < 0.167$, fit the equation:

$$J = 2.6Re^{-0.72}\left(\frac{d}{h}\right)^{0.74} \quad (10)$$

with an average deviation of ±15.7%. Cylinder diameter was used as a characteristic length in calculating *Re*. The above equation can be also written in the form:

$$Sh = 2.6Sc^{0.33}Re^{0.28}\left(\frac{d}{h}\right)^{0.74} \quad (11)$$

When L was used as a characteristic length, an equation similar to Eq. (10) was obtained but with a coefficient of 2.37 instead of 2.6, the average deviation was ±14.8%.

As in the case of Raschig rings, the above equation shows that, that the mass transfer coefficient decreases with increasing bed height and is little affected by cylinder diameter.

It would be of interest to compare Eqs. (7) and (11) with the established equations representing mass transfer at fixed beds. Previous mass transfer data in fixed beds are usually represented by the equation:

$$Sh = a_1Sc^{0.33}Re^{b} \quad (12)$$

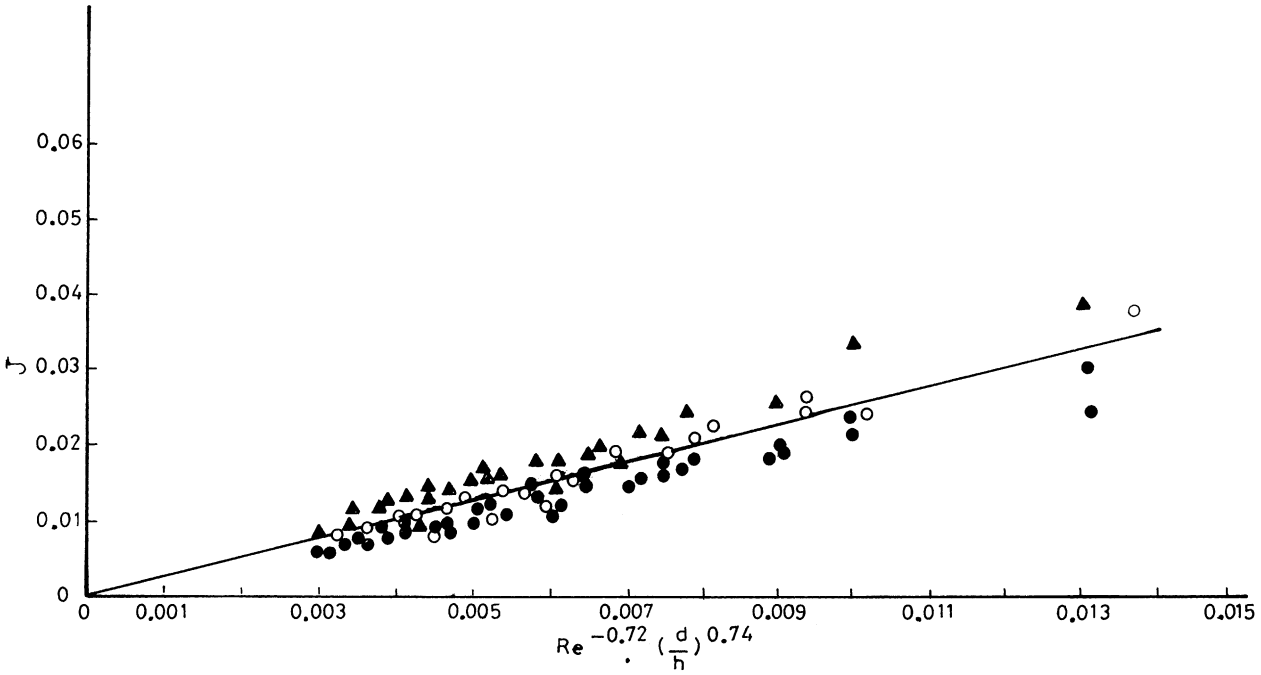

Fig. 5. Mass transfer correlation at a fixed bed of cylinders–plate assembly electrode under single phase flow. *Sc*: (▲) 1729; (●) 1757; (○) 1918.

Where a_1 and b depend on the porous medium and on the range of *Re* investigated. Experiments for forced convection at low *Re* ($0.04 < Re < 55$) provide values of b between 0.174 and 0.35, while at high *Re* the value of b becomes 0.5 or more [16–19]. The mass transfer coefficient predicted from Eqs. (7) and (11), is much lower than the value predicted from Eq. (12) with $a_1 = 0.822$ and $b = 0.62$ as obtained by previous studies for the present range of *Re* [16]. The discrepancy between the present data and the prediction of Eq. (12) may be ascribed to the wall effect and the maldistribution of flow in the beds used in the present work where thin beds of large particle size are used under low solution flow rates. Previous experimental studies on flow in fixed beds [15] show that the flow rate near the wall is higher than that found in the center of the bed. This phenomena is particularly acute with large packing particles in packed beds of small diameter (thickness) at low solution velocities [15]. To avoid the wall effect (channelling), the ratio of the bed diameter to that of the packing particles should be greater than 25 [15]. It seems that under the present conditions the fixed bed receives little flow while the bed walls receives most of the flow. This explains the low *Re* exponents (0.28) obtained in Eqs. (7) and (11) which are consistent with the values obtained for fixed beds at low flow rates ($Re < 55$) [16–19].

3.2. Mass transfer at gas sparged electrodes

Fig. 6 shows that the present mass transfer data for gas sparged vertical plate under the conditions $1546 < Sc < 1757$; $4 \times 10^{-4} < Re\,Fr < 30 \times 10^{-4}$ and $0.929 < h/d_e < 1.857$, fit the equation:

$$J = 0.1(Re\,Fr)^{-0.2}\left(\frac{h}{d_e}\right)^{0.53} \tag{13}$$

with an average deviation of ±17.3%. The above equation predicts lower mass transfer coefficients than those predicted from the semitheoretical equation obtained by combining the surface renewal model and Kolmogoroff theory of isotropic turbulence [20].

$$St \cdot Sc^{0.5} = 0.035(Re\,Fr)^{-0.25} \tag{14}$$

which can be written for the present range of *Sc* in the form:

$$J = 0.115(Re\,Fr)^{-0.25} \tag{15}$$

The prediction of Eq. (14) has proved to match satisfactorily experimental data obtained at relatively high superficial gas velocities [21–24]. Eq. (14) was derived on the assumption that the rising gas bubbles generate radial momentum which destroys the hydrodynamic boundary layer at the electrode surface and induce mass transfer by surface renewal [25]. Under the present conditions where low gas superficial velocities were used ($V_g < 1$ cm/s), it is plausible to assume that the radial momentum is not strong enough to destroy the hydrodynamic boundary layer at the electrode surface and mass is transferred by two simultaneous mechanisms namely: (i) surface renewal mechanism resulting from radial momentum which brings fresh solution to the edge of the hydrodynamic boundary layer; (ii) molecular diffusion inside the hydrodynamic boundary layer which is built along the electrode surface as a result of the axial motion of bubble displaced solution. The dependence of the mass transfer

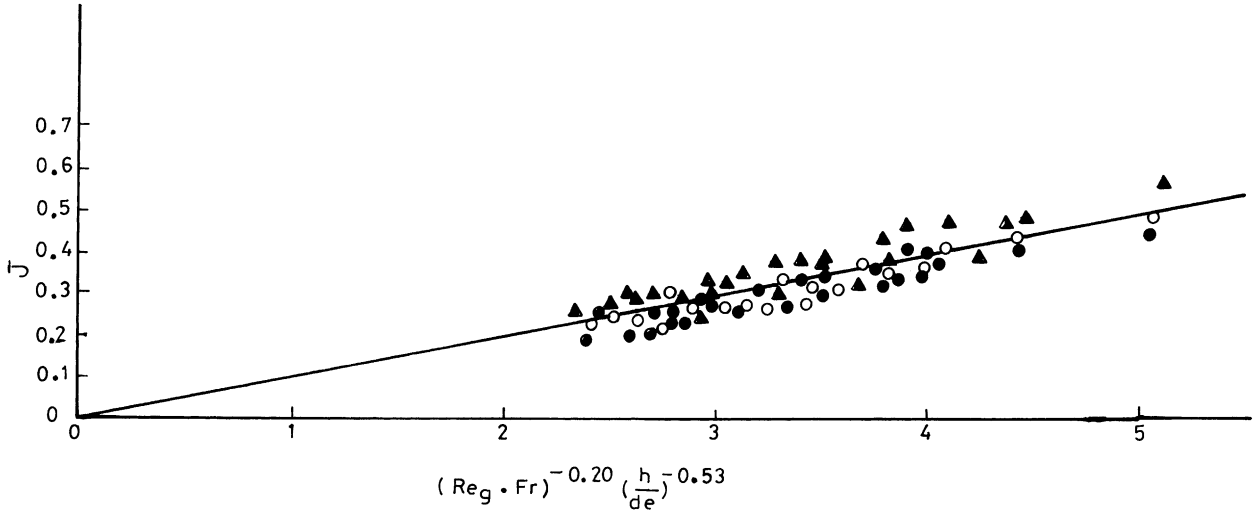

Fig. 6. Mass transfer correlation at gas sparged vertical plate electrode. *Sc*: (●) 1546; (▲) 1697; (○) 1757.

coefficient on electrode height as given by Eq. (13) may lend support to the presence of a hydrodynamic boundary layer. A similar argument has been used to explain the dependence of heat transfer [26] and mass transfer coefficients [27] in gas sparged systems involving high viscosity solutions on the the vertical length of the transfer surface.

Fig. 7 Shows that for fixed bed of Raschig rings–plate assembly the mass transfer data for the conditions $3.9 \times 10^{-4} < ReFr < 30 \times 10^{-4}$, $1536 < Sc < 1884$ and $0.05 < d/h < 0.167$, fit the equation:

$$J = 0.156(ReFr)^{-0.18}\left(\frac{d}{h}\right)^{0.35} \quad (16)$$

with an average deviation of ±7.5%.

For a gas sparged fixed bed of cylinders–plate assembly the mass transfer data (Fig. 8) for the conditions 3.8×

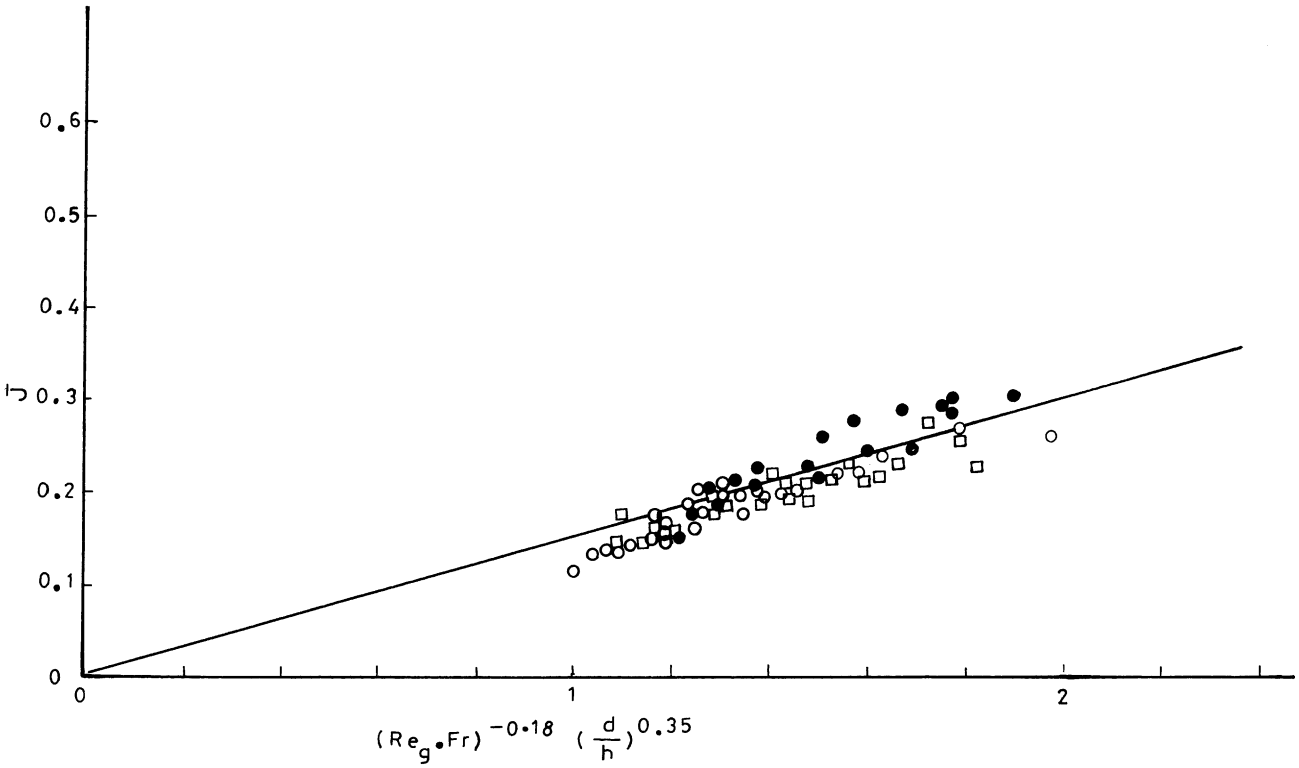

Fig. 7. Mass transfer correlation at gas sparged fixed bed of Raschig rings–plate assembly electrode. *Sc*: (□) 1536; (●) 1697; (○) 1884.

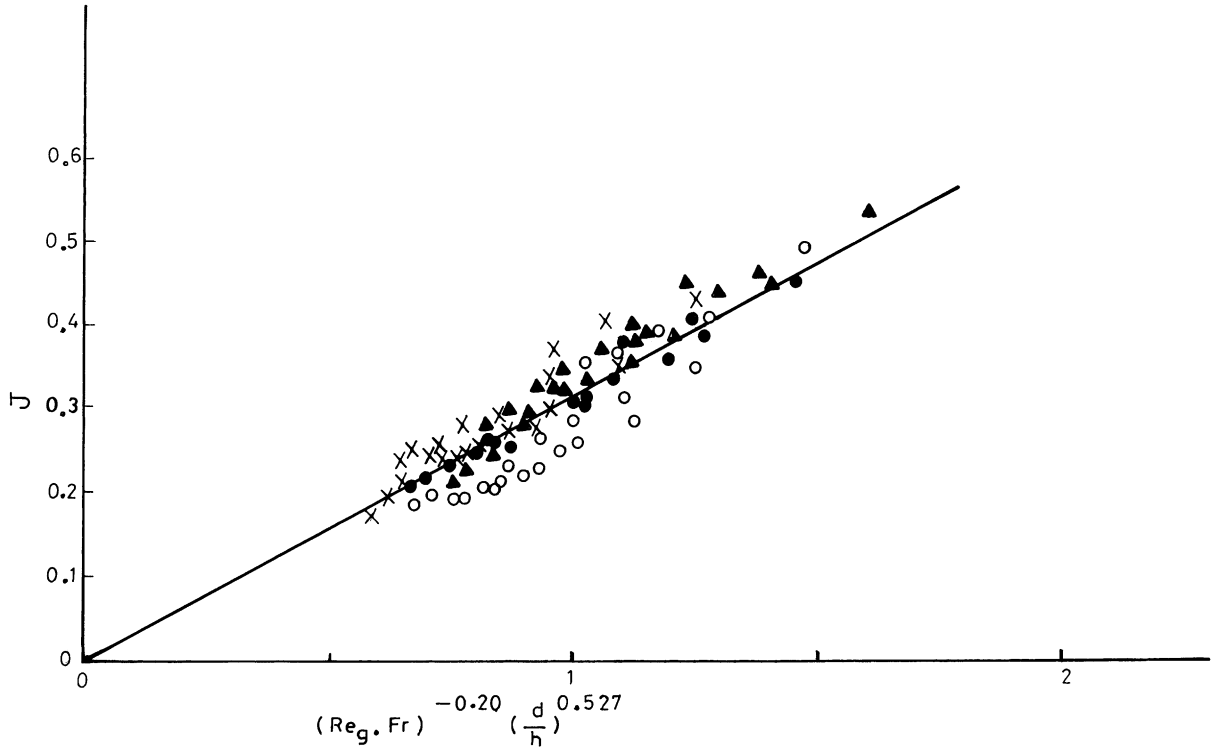

Fig. 8. Mass transfer correlation at gas sparged fixed bed of cylinders–plate assembly electrode. *Sc*: (▲) 1536; (●) 1697; (X) 1823; (○) 1884.

$10^{-4} < Re\,Fr < 30.1 \times 10^{-4}$; $1536 < Sc < 1834$ and $0.05 < d/h < 0.167$ were found to fit the equation:

$$J = 0.28(Re\,Fr)^{-0.2}\left(\frac{d}{h}\right)^{0.527} \quad (17)$$

with an average deviation of ±8.4%.

Particle diameter was used as a characteristic length in calculating *Re* and *Fr* in case of bed–plate assembly.

The high mass transfer coefficient obtained for gas sparged bed–plate assembly compared to that obtained at the plate for a given superficial gas velocity may be attributed to the fact that beside the turbulence and the radial momentum induced by the rising bubbles [25], mass transfer is enhanced also at the fixed bed–plate assembly by the collision of the rising bubbles with the bed particles with a consequent disturbance of the diffusion layer.

3.3. Two phase mass transfer

Fig. 9 shows that the two phase mass transfer data at plate electrode for the conditions $1823 < Sc < 2084$; $39.5 < Re_g < 334$; $364 < Re < 2668$ and $0.928 < h/d_e < 1.857$, fit the equation:

$$Sh = 1.75Sc^{0.33}Re_g^{0.25}Re^{0.5}\left(\frac{h}{d_e}\right)^{0.23} \quad (18)$$

with an average deviation of ±15%.

Fig. 10 shows that the two phase mass transfer data at a Raschig rings–plate assembly for the conditions $1478 < Sc < 2026$;$4.2 < Re_g < 28.9$; $35 < Re_L < 232$ and $0.05 < d/h < 0.167$, fit the equation:

$$Sh = 15Sc^{0.33}Re_g^{0.15}Re^{0.17}\left(\frac{d}{h}\right)^{0.55} \quad (19)$$

with an average deviation of ±8.1%.

Fig. 11 shows that the two phase mass transfer data at a bed of cylinders–plate assembly for the conditions $1981 < Sc < 2104$; $2.95 < Re_g < 26.3$; $34.6 < Re_L < 217$ and $0.05 < d/h < 0.167$, fit the equation:

$$Sh = 6Sc^{0.33}Re_g^{0.17}Re^{0.08}\left(\frac{d}{h}\right)0.384 \quad (20)$$

with an average deviation of ±11%.

The higher dependence of the mass transfer coefficient on the solution velocity than the gas velocity in case of the plate electrode as shown by Eq. (18) is consistent with the finding of Economou and Alkire [11] despite the higher range of V_L and V_g used by these authors who studied the rate of mass transfer in the fully developed region of a parallel plate reactor. Eqs. (19) and (20) show that contrary to the case of flat plate, gas velocity assumes more important role in determining the mass transfer coefficient than solution velocity especially in case of cylinder packing, this may be attributed to:

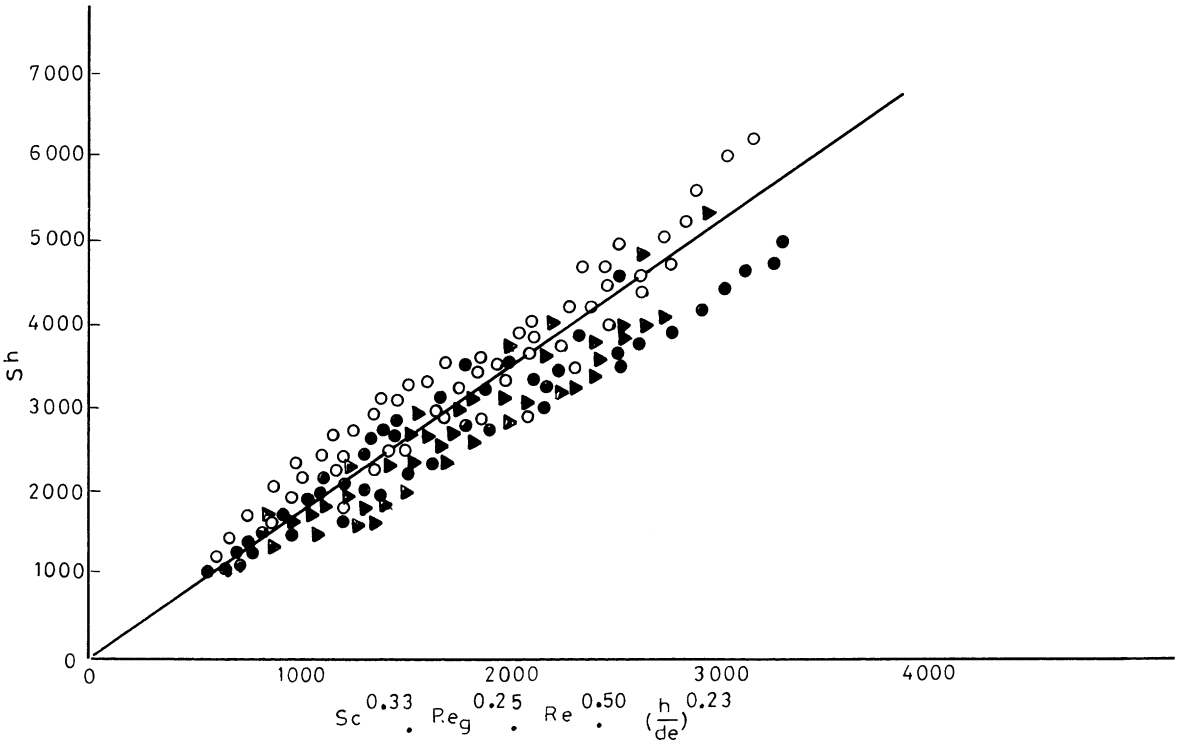

Fig. 9. Two phase mass transfer correlation at a vertical plate. *Sc*: (○) 1823; (▲) 1982; (●) 2084.

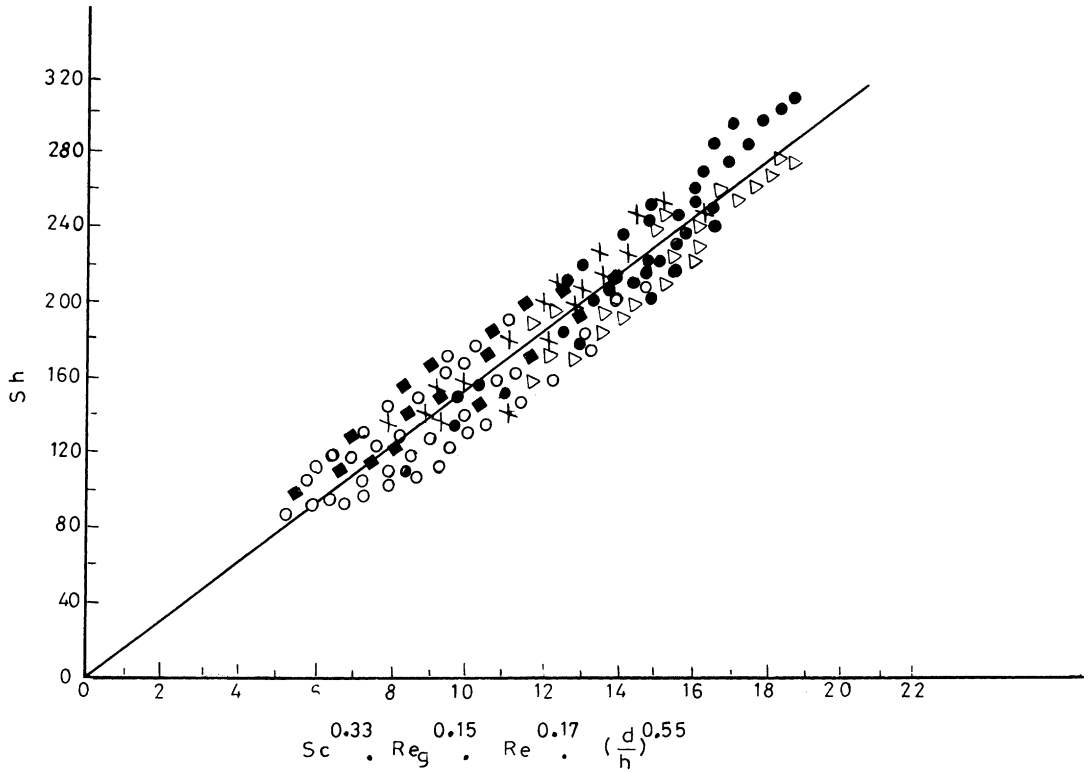

Fig. 10. Two phase mass transfer correlation at a fixed bed of Raschig rings–plate assembly electrode. *Sc*: (X) 1478; (●) 1697; (○) 1795; (△) 1884; (■) 2026.

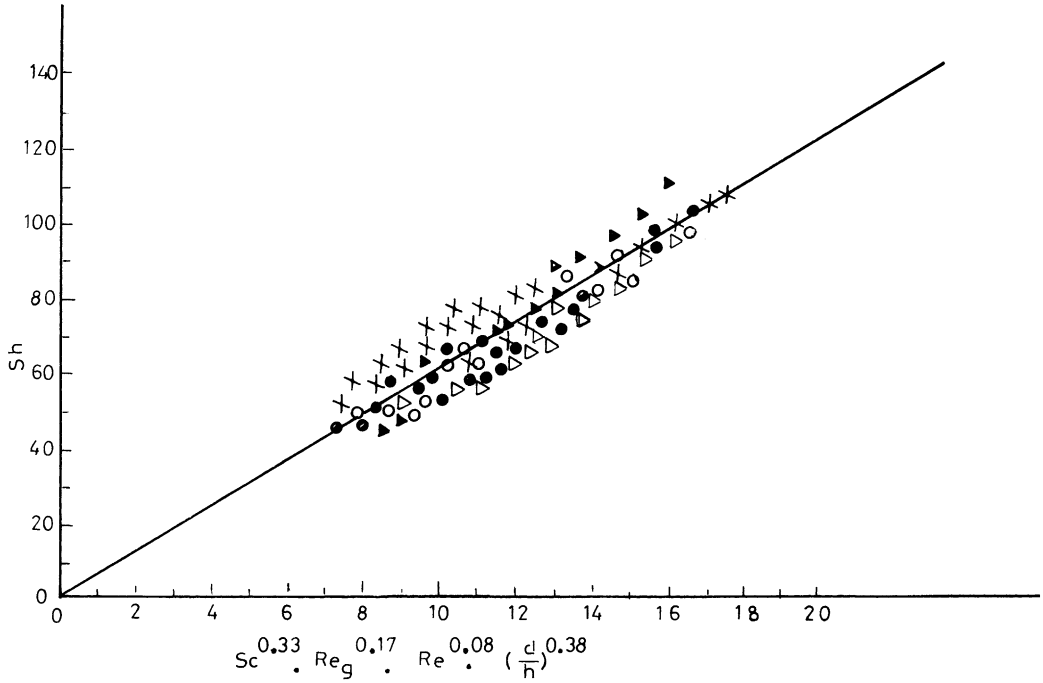

Fig. 11. Two phase mass transfer correlation at a fixed bed of cylinders–plate assembly electrode. *Sc*: (●) 1884; (▲) 1982; (X) 2026; (○) 2084; (△) 2104.

(i) the channelling effect divert part of the solution from the bed to the wall region. It seems that this effect is more pronounced in case of cylinder packing where the porosity is less than in case of Raschig rings;
(ii) in addition to the usual enhancing effects of gas bubbles such as decreasing the flow area of the solution which leads to increasing solution velocity, radial momentum transfer and turbulence generation in the bubble wake, a peculiar effect is displayed in case of fixed bed, namely collision of the rising bubbles with the packing particles with a consequent disruption of the diffusion layer, this effect is absent in case of the plate electrode.

3.4. Performance of the bed–plate assembly compared to the plate electrode

To assess the improvement in the performance of the parallel plate electrochemical reactor as a result of packing the interelectrode gap with metallic Raschig rings, and cylinders, two indicators were used, namely: (1) the ratio $(KA)_{bed}/(KA)_{plate}$ which reflects the productivity ratio; (2) electrical power consumption in kWh/kg of deposited copper at the limiting current. The volumetric mass transfer

Table 2
Effect of solution velocity on the ratio $(KA)_{bed-plate\ assembly}/(KA)_{plate}$ under single phase flow

Solution velocity (cm/s)	$(KA)_{bed\ of\ rings-plate}/(KA)_{plate}$	$(KA)_{bed\ of\ cylinders-plate}/(KA)_{plate}$
0.68	4.14	4.17
1.15	3.975	4.125
1.46	3.38	3.4
1.78	3.16	3
2.08	3.03	2.8
2.51	2.8	2.64

$CuSO_4$ conc., 0.05 M; bed height, 12 cm; particle diameter, 0.6 cm.

Table 3
Effect of superficial gas velocity on the ratio $(KA)_{bed-plate\ assembly}/(KA)_{plate}$ under gas sparging

Superficial gas velocity (cm/s)	$(KA)_{bed\ of\ cylinders-plate}/(KA)_{plate}$	$(KA)_{bed\ of\ cylinders-plate}/(KA)_{plate}$
0.16	6.67	9.259
0.2	6.67	9.12
0.23	7	9.55
0.26	7.22	9.59
0.29	7.1	9.5
0.31	7.19	9.38

$CuSO_4$ conc., 0.05 M; bed height, 12 cm; particle diameter, 0.6 cm.

Table 4
Effect of solution velocity on the ratio $(KA)_{bed-plate}/(KA)_{plate}$ under two phase flow

Solution velocity (cm/s)	$(KA)_{bed\ of\ rings-plate}/(KA)_{plate}$	$(KA)_{bed\ of\ cylinders-plate}/(KA)_{plate}$
0.684	6.8	6.2
1.15	5.2	4.7
1.46	4.7	4.2
1.78	4.4	3.96
2.08	4.2	3.8
2.51	3.4	3.2

$CuSO_4$ conc., 0.05 M; bed height, 12 cm; particle diameter, 0.6 cm; superficial gas velocity, 0.31 cm/s.

Table 5
Comparison of the electrical energy consumption for different types of electrodes under single phase forced convection

Solution velocity (cm/s)	Vertical plate electrode			Vertical bed–plate of Raschig rings electrode			Vertical bed–plate of cylinders electrode		
	Cell voltage (V)	Limiting current (A)	Energy (kWh/kg)	Cell voltage (V)	Limiting current (A)	Energy (kWh/kg)	Cell voltage (V)	Limiting current (A)	Energy (kWh/kg)
0.684	0.50	0.36	0.42	0.3	1.49	0.25	0.40	1.5	0.34
1.154	0.55	0.40	0.55	0.35	1.59	0.29	0.50	1.65	0.42
1.46	0.60	0.502	0.60	0.40	1.69	0.34	0.55	1.7	0.47
1.78	0.65	0.57	0.65	0.45	1.80	0.38	0.60	1.75	0.51
2.08	0.70	0.64	0.70	0.50	1.4	0.42	0.65	1.8	0.55
2.509	0.75	0.72	0.75	0.55	2.02	0.46	0.70	1.90	0.60

$CuSO_4$ conc., 0.05 M; electrode height, 12 cm; cylinder or ring diameter, 0.6 cm.

Table 6
Comparison of the electrical energy consumption for different types of electrodes under gas sparging

Solution velocity (cm/s)	Vertical plate electrode			Vertical bed–plate of Raschig rings electrodes			Vertical bed–plate of cylinders electrode		
	Cell voltage (V)	Limiting current (A)	Energy (kWh/kg)	Cell voltage (V)	Limiting current (A)	Energy (kWh/kg)	Cell voltage (V)	Limiting current (A)	Energy (kWh/kg)
0.162	0.75	0.27	0.63	0.55	1.8	0.46	0.65	2.5	0.55
0.203	0.80	0.285	0.68	0.60	1.9	0.51	0.70	2.6	0.59
0.233	0.85	0.288	0.72	0.65	2.05	0.55	0.75	2.75	0.63
0.2619	0.95	0.292	0.76	0.70	2.1	0.59	0.80	2.8	0.68
0.2899	0.95	0.31	0.80	0.75	2.2	0.63	0.85	2.95	0.72
0.3125	1.0	0.32	0.85	0.80	2.3	0.68	0.90	3.0	0.76

$CuSO_4$ conc., 0.05 M; electrode height, 12 cm; cylinder or ring diameter, 0.6 cm.

coefficient (KA) was calculated from the experimentally determined limiting current using Eq. (3). Tables 2–4 show that the productivity of the fixed bed–plate assembly is higher than that of the parallel plate electrochemical reactor by a factor ranging from 2.6 to 9.6 depending on the operating conditions.

Tables 2–4 show that the ratio $(KA)_{bed}/(KA)_{plate}$ for gas sparging is higher than that in case of single phase flow and two phase flow probably because of the adverse effects of channelling which is likely to take place in case of single and two phase flow under the present conditions where relatively thin fixed bed is used. The better performance of gas sparged fixed bed of cylinders compared to that of gas sparged fixed bed of Raschig rings as shown in Table 3 may be attributed to the fact that the inner surface of the horizontally oriented rings are not accessible to gas bubbles, i.e mass transfer inside these horizontal rings takes place mainly by natural convection.

Tables 5–7 show that the cell voltage and electrical energy consumption decrease in the order: plate electrode, bed of cylinders, bed of Raschig rings. The low cell voltage and energy consumption of the bed electrodes compared to the parallel plate electrode may be ascribed to the lower cell resistance and the lower ohmic drop (IR) in case of bed electrodes. The high conductivity of the bed cell compared to that of the parallel electrode arises from the fact that metallic packing particles extends the cathode surface towards the anode, i.e decreases the interelectrode gap. In the mean

Table 7
Comparison of the electrical energy consumption for different electrodes under two phase flow

Solution Vertical (cm/s)	Vertical bed–plate of electrode			Vertical bed–plate of Raschig rings electrode			Vertical bed–plate of cylinders electrode		
	Cell voltage (V)	Limiting current (A)	Energy (kWh/kg)	Cell voltage (V)	Limiting current (A)	Energy (kWh/kg)	Cell voltage (V)	Limiting current (A)	Energy (kWh/kg)
0.68	2.15	0.76	1.82	1.85	5.2	1.57	2	4.7	1.7
1.15	2.25	1.02	1.91	1.9	5.3	1.61	2.05	4.8	1.74
1.46	2.3	1.15	1.95	1.95	5.45	1.65	2.1	4.9	1.78
1.785	2.35	1.26	2	2	5.5	1.7	2.15	5	1.82
2.09	2.4	1.34	2.04	2.05	5.6	1.74	2.2	5.15	1.87
2.51	2.45	1.64	2.08	2.1	5.65	1.78	2.25	5.2	1.91

$CuSO_4$ conc., 0.05 M; electrode height, 12 cm; cylinder or ring diameter, 0.6 cm; superficial gas velocity, 0.31 cm/s.

time, it seams that the increase in cell conductivity resulting from the decrease in electrode separation outweighs the decrease in the effective solution conductivity (K_{eff}) caused by the presence of the packing material according to the equation [1]:

$$K_{eff} = K_o \varepsilon^{1.5} \quad (21)$$

4. Conclusion

1. The present study have shown that filling the interelectrode gap of the parallel plate electrochemical reactor with a packing metallic Raschig rings or cylinders separated from the counter electrode by a diaphragm or perforated separator would offer the following advantages over the parallel plate electrochemical reactor:
   (i) the productivity of the reactor increases by a factor ranging from 2.8 to 9.6 depending mainly on the prevailing hydrodynamic conditions;
   (ii) electrical energy consumption in kWh/kg decreases below that of the unpacked parallel plate reactor.

   The present fixed bed flow-by electrochemical reactor can find applications in waste-water treatment and electrochemical reactions involving simultaneous gas absorption and diffusion controlled or partially diffusion controlled electrochemical reactions. However, before using the proposed reactor in practice, a pilot plant study of the negative effect of increasing pressure and pumping energy is needed to make sure that the advantages of the reactor outweigh the increase in pressure drop.
2. Mass transfer measurement has revealed that the present thin fixed beds built of relatively large particles and supported by a vertical feeder plate differ in their mass transfer behaviour from traditional thick fixed beds. The present dimensionless equations can be used in the design and operation of flow-by fixed bed electrochemical reactors similar to that used in the present work.

References

[1] F. Walsh, A First Course in Electrochemical Engineering, The Electrochemical Consultancy, Hants, UK, 1993.
[2] G.H. Sedahmed, Can. J. Chem. Eng. 74 (1996) 487.
[3] G.H. Sedahmed, Can. J. Chem. Eng. 64 (1986) 75.
[4] C. Oloman, A.P. Watkinson, Can. J. Chem. Eng. 54 (1976) 312.
[5] M.M. Nassar, A.M. Al-Taweel, G.D. Mackay, A.F. Mcmillan, G.H. Sedahmed, Surf. Technol. 20 (1983) 83.
[6] K. Scott, Bull. Electrochem. 9 (1993) 170.
[7] D.J. Pickett, B.R. Stanmore, J. Appl. Electrochem. 5 (1975) 95.
[8] V.A. Ettel, B.V. Tilak, A.S. Gendron, J. Electrochem. Soc. 121 (1974) 867.
[9] N. Ibl, R. Kind, E. Adam, Ann. de Quim. 71 (1975) 1008.
[10] L. Sigrist, O. Dossenbach, N. Ibl, Int. J. Heat Mass Transfer 22 (1979) 1393.
[11] D. Economou, R. Alkire, J. Electrochem. Soc. 132 (1985) 601.
[12] A.I. Vogel, A Textbook of Quantitative Inorganic Analysis, 3rd Edition, Longmans, London, 1961.
[13] A. Findlay, J.K. Kitchener, Pratical Physical Chemistry, Longmans, London, 1965.
[14] J.R. Selman, C.W. Tobias, Adv. Chem. Eng. 10 (1978) 211.
[15] Y.Y. Wang, Principles of packed-bed electrochemical reactors, in: N.P. Cheremisinoff (Ed.), Handbook of Heat and Mass Transfer, Vol. 2, Gulf Publishing Co., London, 1986.
[16] D. Seguin, A. Montillet, D. Brunjail, J. Comiti, Chem. Eng. J. 63 (1996) 1.
[17] A.J. Karabelas, T.H. Wegner, T.J. Hanratty, Chem. Eng. Sci. 26 (1971) 1581.
[18] I. Colquhoun, J. Stepanek, Chem. Eng. 108 (2) (1974).
[19] S.N. Upadhay, B.K.D. Agrawal, D.R. Singh, J. Chem. Eng. Jpn. 8 (1975) 413.
[20] G.H. Sedahmed, J. Appl. Electrochem. 15 (1985) 777.
[21] O.H. Sedahmed, A.Y. Hosny, O.A. Fadally, I.M. El-Mekkawy, J. Appl. Electrochem. 24 (1994) 139.
[22] J. St-Pierre, D.L. Piron, J. Electrochem. Soc. 139 (1992) 105.
[23] M.M. Zaki, I. Nirdosh, G.H. Sedahmed, Can. J. Chem. Eng. 75 (1997) 333.
[24] M.M. Zaki, I. Nirdosh, O.H. Sedahmed, Can. J. Chem. Eng. 78 (2000) 1096.
[25] W.D. Deckwer, Chem. Eng. Sci. 35 (1980) 1341.
[26] D.A. Lewis, R.W. Field, A.M. Xavier, D. Edwards, Trans. I. Chem. E 60 (1982) 40.
[27] G.H. Sedahmed, M.S. Abdo, M.A. Kamal, O.A. Fadally, H.M. Osman, Chem. Eng. Process. 40 (2001) 195.